Integrated switchable reflector based on periodically poled acoustic superlattice $LiNbO_3$

2002 J. Phys. D: Appl. Phys. 35 1414

(http://iopscience.iop.org/0022-3727/35/12/319)

INSTITUTE OF PHYSICS PUBLISHING JOURNAL OF PHYSICS D: APPLIED PHYSICS
J. Phys. D: Appl. Phys. **35** (2002) 1414–1421 PII: S0022-3727(02)29558-3

Integrated switchable reflector based on periodically poled acoustic superlattice $LiNbO_3$

Xue-jin Zhang, Yong-yuan Zhu, Yan-feng Chen, Zhi-liang Wan, Yan-qing Lu and Nai-ben Ming

National Laboratory of Solid State Microstructures, Nanjing University, Nanjing 210093, People's Republic of China

E-mail: yyzhu@nju.edu.cn

Received 10 October 2001, in final form 5 March 2002
Published 31 May 2002
Online at stacks.iop.org/JPhysD/35/1414

Abstract
In this paper, an integrated acoustic device made of the periodically poled superlattice $LiNbO_3$ crystals is discussed, which includes a transducer, an acoustic switch, and a transmission medium. The influence of the DC bias on the propagation of acoustic waves in the switch part is analysed theoretically. The results show that the greater the amplitude of DC bias, the greater the reflectivity. The distribution of the reflection spectra depends on the thickness of domains. The acoustic bandgaps increase with the DC bias but decrease with the number of periods. The design of the device has the advantage that monolithic integration can be realized with the largest electromechanical coefficient to be used.

1. Introduction

The periodically poled superlattice $LiNbO_3$ (PPLN) has been researched and applied widely. In PPLN, the odd-rank tensors, such as the nonlinear optical coefficient, electrooptic coefficient, and piezoelectric coefficient, will change their signs periodically. Because of this, it has been used for quasi-phase-matched (QPM) second harmonic generation [1], electrooptic modulation (EOM) [2–4] and bulk acoustic wave generation [5–11]. In general, the value of even-rank tensor is unaltered with the superlattice structure. But it has been proved that both the dielectric tensor and the elastic tensor can be modulated by an external electric field through nonlinearity or coupled physical effects, such as electroacoustic and electrooptic effects [12]. Thus new inhomogeneity will be brought about to the propagation of light and acoustic waves compared with those without the application of an external electric field.

We named superlattices as optical superlattices (OSLs), and acoustic superlattices (ASLs) according to their different applications in the fields of optics and acoustics. ASLs may be subdivided into 'in-line field' and 'crossed-field' schemes [13]. The former is characterized by an applied electric field parallel to the propagation wavevector and the latter by an applied electric field perpendicular to the propagation wavevector. The 'crossed-field' scheme has such advantages that devices, such as the acoustooptic modulators and acoustooptic deflectors, can be realized without the use of bonds between the transducers and transmission medium. In this case, acoustic waves will not be impeded by bonds, so the spectral transmission properties of acoustic waves can be improved greatly [14].

So far, in applications of ASLs, resonators [5, 15], transducers [6, 11, 16], and acoustic–optic tunable filters (AOTFs) [17] have come out. In this paper, we will introduce a new application (acoustic switch) of 'cross-field' ASLs $LiNbO_3$ (ASLLN), which is integrated together with the transducer and the transmission medium.

The paper is dealt with as follows. Theoretical analysis and calculation about the acoustic switch is described in section 2. The reflectivity of acoustic waves is discussed in section 3, and conclusions are briefly summarized in section 4.

2. Theoretical analysis

We propose a monolithic integration device. In the device, an acoustic switch is integrated together with a transducer and a transmission medium. In these three parts, the transducer and the acoustic switch are made of ASLLN, and the transmission

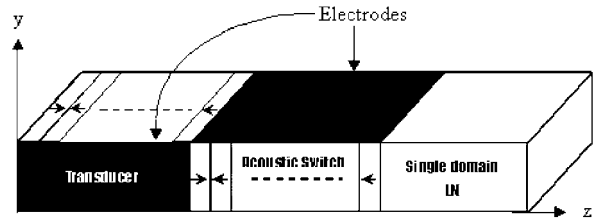

Figure 1. A schematic diagram of an integrated device including three parts: a transducer, an acoustic switch, and a transmission medium. Arrows along positive z indicate positive domains and those along negative z represent negative ones.

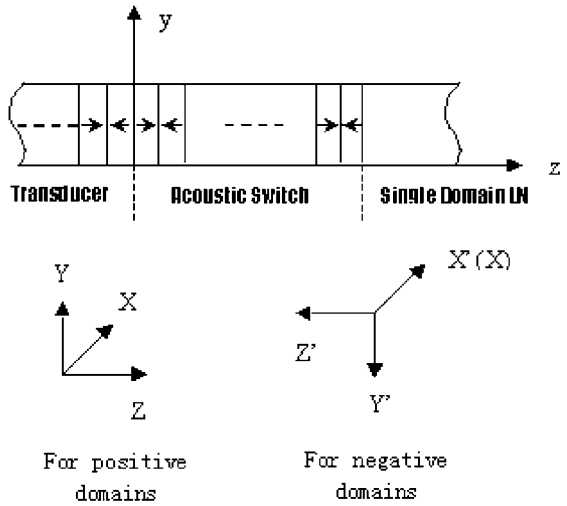

Figure 2. The coordinate systems for positive and negative domains.

medium is a single domain $LiNbO_3$. The positive and negative domains are arranged along the Z-axis. The electrodes in the transducer part are coated on X-faces while those in the acoustic switch part on Y-faces. The schematic diagram of the device is shown in figure 1.

$LiNbO_3$ (LN) is a ferroelectric crystal with the symmetry of 3 m. The crystallographic coordinate system rotates 180° around the crystal X-axis in the negative domain compared with that in the positive domain [18], which is shown in figure 2. In this case, all elements of the odd-rank tensors will change signs from one domain to the next. That is, the odd-rank tensors will be modulated in the positive and negative domains. In what follows we prove that the velocities of sound waves will no longer be constant in the ASLLN under an external electric field. It will result in the reflection of acoustic waves propagating along ASLLN. This is the fundamental principle of our acoustic switch.

2.1. Thermodynamic description of elastoelectric effect

The thermodynamic potentials are generally used for describing physical properties of materials. We consider thermodynamic potential $H_{\text{el.}}$, electric enthalpy, the change of which is [19]

$$\mathrm{d}H_{\text{el.}} = T_{ij}\mathrm{d}S_{ij} - D_m\mathrm{d}E_m + \tau\mathrm{d}\sigma \quad (i, j, m = 1, 2, 3), \tag{1}$$

where D_m, E_m, T_{ij}, S_{ij}, τ and σ are the electric displacement, electric field, stress, strain, temperature and entropy, respectively;

$$T_{ij} = \left(\frac{\partial H_{\text{el.}}}{\partial S_{ij}}\right)_{E,\sigma}, \qquad D_m = -\left(\frac{\partial H_{\text{el.}}}{\partial E_m}\right)_{S,\sigma}, \qquad \tau = \left(\frac{\partial H_{\text{el.}}}{\partial \sigma}\right)_{E.S}. \tag{2}$$

These come from the total differential form of equation (1). The following relationship can be easily got from equation (2):

$$\left(\frac{\partial T_{ij}}{\partial E_m}\right)_{\sigma,S} = -\left(\frac{\partial D_m}{\partial S_{ij}}\right)_{\sigma,E}. \tag{3}$$

It is supposed that $\mathrm{d}\sigma = 0$, i.e. an adiabatic process considered for crystals. Let us give the following definitions in advance:

$$C_{ijkl} = \left(\frac{\partial T_{ij}}{\partial S_{kl}}\right)_{\sigma,E} = \left(\frac{\partial^2 H_{\text{el.}}}{\partial S_{ij}\,\partial S_{kl}}\right)_{E,\sigma}, \tag{4}$$

$$C_{ijklpq} = \left(\frac{\partial^2 T_{ij}}{\partial S_{kl}\,\partial S_{pq}}\right)_{\sigma,E} = \left(\frac{\partial^3 H_{\text{el.}}}{\partial S_{ij}\,\partial S_{kl}\,\partial S_{pq}}\right)_{E,\sigma}, \tag{5}$$

$$e_{mij} = \left(\frac{\partial D_m}{\partial S_{ij}}\right)_{\sigma} = -\left(\frac{\partial T_{ij}}{\partial E_m}\right)_{\sigma} = -\left(\frac{\partial^2 H_{\text{el.}}}{\partial E_m\,\partial S_{ij}}\right)_{\sigma}, \tag{6}$$

$$g_{mijkl} = \left(\frac{\partial^2 D_m}{\partial S_{ij}\,\partial S_{kl}}\right)_{\sigma} = -\left(\frac{\partial^2 T_{ij}}{\partial S_{kl}\,\partial E_m}\right)_{\sigma} = -\left(\frac{\partial^3 H_{\text{el.}}}{\partial S_{ij}\,\partial S_{kl}\,\partial E_m}\right)_{\sigma}, \tag{7}$$

$$Q_{ijmn} = \left(\frac{\partial^2 D_m}{\partial S_{ij}\,\partial E_m}\right)_{\sigma} = -\left(\frac{\partial^2 T_{ij}}{\partial E_m\,\partial E_n}\right)_{\sigma} = -\left(\frac{\partial^3 H_{\text{el.}}}{\partial S_{ij}\,\partial E_m\,\partial E_n}\right)_{\sigma}, \tag{8}$$

where C_{ijkl}, C_{ijklpq}, e_{mij}, g_{mijkl} and Q_{ijmn}, respectively, represent the second-order elastic, third-order elastic, piezoelectric, elastoelectric and electrostriction coefficients. Then

$$\begin{aligned} T_{ij} &= \left(\frac{\partial H_{\text{el.}}}{\partial S_{ij}}\right)_{E,\sigma} \\ &= \left(\frac{\partial T_{ij}}{\partial S_{kl}}\right)_{E,\sigma} S_{kl} + \left(\frac{\partial T_{ij}}{\partial E_m}\right)_{S,\sigma} E_m \\ &\quad + \frac{1}{2}\left(\frac{\partial^2 T_{ij}}{\partial S_{kl}\,\partial S_{pq}}\right)_{E,\sigma} S_{kl}S_{pq} + \left(\frac{\partial^2 T_{ij}}{\partial S_{kl}\,\partial S_m}\right)_{\sigma} S_{kl}E_m \\ &\quad + \frac{1}{2}\left(\frac{\partial^2 T_{ij}}{\partial E_m\,\partial E_n}\right)_{S,\sigma} E_m E_n \\ &= C_{ijkl}S_{kl} - e_{mij}E_m + \tfrac{1}{2}C_{ijklpq}S_{kl}S_{pq} \\ &\quad - g_{mijkl}E_m S_{kl} - \tfrac{1}{2}Q_{ijmn}E_m E_n. \end{aligned} \tag{9}$$

where T_{ij}, E_m, S_{kl} and S_{pq} are reckoned relative to their values at zero stress and field. The members higher than the second-order ones in this expanding expression are not taken into consideration. From the above equation, the elastic moduli of crystals under the electric field influence change to

$$C^E_{ijkl} = C_{ijkl} - g_{mijkl}E_m \qquad (i, j, k, l, m = 1, 2, 3). \tag{10}$$

Thanks to the symmetry, equation (10) can be simplified to

$$C^E_{IJ} = C_{IJ} - g_{mIJ}E_m \quad (m = 1, 2, 3 \text{ and } I, J = 1, 2, 3, 4, 5, 6). \tag{11}$$

For the LN crystal,

$$[C_{IJ}^{E}] = \begin{bmatrix} C_{11} & C_{12} & C_{13} & C_{14} & 0 & 0 \\ C_{12} & C_{11} & C_{13} & -C_{14} & 0 & 0 \\ C_{13} & C_{13} & C_{33} & 0 & 0 & 0 \\ C_{14} & -C_{14} & 0 & C_{44} & 0 & 0 \\ 0 & 0 & 0 & 0 & C_{44} & C_{14} \\ 0 & 0 & 0 & 0 & C_{14} & C_{66} \end{bmatrix}, \quad (12)$$

where $C_{66} = (C_{11} - C_{12})/2$, and C_{11}, C_{12}, C_{13}, C_{14}, C_{33} and C_{44} are constants. The form of $[C_{IJ}^{E}]$ is then as shown in figure 3(*a*) (equation (13)).

In the bulk–wave acoustic switch part of the integrated device, E_1 and E_3 are considered to be zero because the electrodes are on the Y-faces. The matrix $[C_{IJ}^{E}]$ reduces to the one shown in figure 3(*b*) (equation (14)).

2.2. Acoustic wave propagating along the Z-axis in the device

In the transducer part, as mentioned before, an alternate external electric field is applied on the X-faces. That is $E_1 \neq 0$. In this case, there are only X-polarized shear waves being excited and propagating along the Z-axis [9]. In our case, all acoustic interfaces are parallel to the XY plane, so the acoustic waves are propagating along the Z-axis in the acoustic switch and the transmission medium from Snell's law considerations.

Generally three kinds of waves, which can be derived from Christoffel's equation, could exist in the acoustic switch due to anisotropy of LN crystals. But in our case what kinds of waves will exist there when the X-polarized shear waves are transmitted to the acoustic switch? Such a problem can be solved based on the boundary conditions.

The stress must be the same on either side of the interface. At the same time, the particle velocity must be continuous across the interface. These are acoustic boundary conditions, which can be written as [20]

$$\begin{aligned} \boldsymbol{v} &= \boldsymbol{v}', \\ \boldsymbol{T} \cdot \hat{\boldsymbol{n}} &= \boldsymbol{T}' \cdot \hat{\boldsymbol{n}}, \end{aligned} \quad (15)$$

where $\hat{\boldsymbol{n}}$ is the unit vector normal to the interface. The primed objects in equation (15) are the corresponding parameters on the other side of the interface.

$$[C_{IJ}^{E}] = \begin{bmatrix} c_{11} + g_{211}E_2 + g_{311}E_3 & c_{12} - (g_{222} + g_{211})E_2 + g_{312}E_3 & c_{13} - g_{223}E_2 + g_{313}E_3 & c_{14} + g_{214}E_2 + g_{314}E_3 & g_{244}E_1 & (3g_{222} - g_{211})E_1 \\ c_{12} - (g_{222} + g_{221})E_2 + g_{312}E_3 & c_{11} + g_{222}E_2 + g_{313}E_3 & c_{13} - g_{223}E_2 + g_{313}E_3 & -c_{14} + g_{224}E_2 - g_{314}E_3 & g_{214}E_1 & (3g_{211} + g_{222})E_1 \\ c_{13} - g_{223}E_2 + g_{313}E_3 & c_{13} - g_{223}E_2 + g_{314}E_3 & c_{33} + g_{333}E_3 & g_{234}E_2 & g_{234}E_1 & -2g_{223}E_1 \\ c_{14} + g_{214}E_2 + g_{314}E_3 & -c_{14} + g_{224}E_2 - g_{314}E_3 & g_{234}E_2 & c_{44} + g_{244}E_2 + g_{344}E_3 & -2g_{244}E_1 & (g_{224} - g_{214})E_1 \\ g_{224}E_1 & g_{214}E_1 & g_{234}E_1 & -2g_{244}E_1 & c_{44} - g_{244}E_2 + g_{344}E_3 & c_{14} + (g_{244} - g_{214})E_2 + g_{314}E_3 \\ (3g_{222} - g_{211})E_1 & (3g_{211} + g_{222})E_1 & -2g_{223}E_1 & (g_{224} - g_{214})E_1 & c_{14} + (g_{224} - g_{214})E_2 + g_{314}E_3 & c_{66} - 2(g_{222} + g_{211})E_2 + \frac{1}{2}(g_{311} - g_{312})E_3 \end{bmatrix} \quad (13)$$

Figure 3(a).

$$[C_{IJ}^{E}] = \begin{bmatrix} C_{11} + g_{211}E_2 & C_{12} - (g_{222} + g_{211})E_2 & C_{13} - g_{223}E_2 & C_{14} + g_{214}E_2 & 0 & 0 \\ C_{12} - (g_{222} + g_{221})E_2 & C_{11} + g_{222}E_2 & C_{13} - g_{223}E_2 & -C_{14} + g_{224}E_2 & 0 & 0 \\ C_{13} - g_{223}E_2 & C_{13} - g_{223}E_2 & C_{33} & g_{234}E_2 & 0 & 0 \\ C_{14} + g_{214}E_2 & -C_{14} + g_{224}E_2 & g_{234}E_2 & C_{44} + g_{244}E_2 & 0 & 0 \\ 0 & 0 & 0 & 0 & C_{44} - g_{244}E_2 & C_{14} + (g_{244} - g_{214})E_2 \\ 0 & 0 & 0 & 0 & C_{14} + (g_{224} - g_{214})E_2 & C_{66} - 2(g_{222} + g_{211})E_2 \end{bmatrix} \quad (14)$$

Figure 3(b).

It is necessary to refer all field components to the same coordinate system. In equation (15), $\hat{n} = \hat{z}$, as shown in figure 2. Thereafter we get six boundary conditions

$$\begin{aligned} v_x &= v'_x, \qquad v_y = v'_y, \\ v_z &= v'_z, \qquad T_{xz} = T'_{xz}, \\ T_{yz} &= T'_{yz}, \qquad T_{zz} = T'_{zz}. \end{aligned} \tag{16}$$

The coordinate systems of the positive and negative domain are associated with a coordinate transformation matrix,

$$\begin{bmatrix} X \\ Y \\ Z \end{bmatrix} = \begin{bmatrix} 1 & 0 & 0 \\ 0 & -1 & 0 \\ 0 & 0 & -1 \end{bmatrix} \begin{bmatrix} X' \\ Y' \\ Z' \end{bmatrix}. \tag{17}$$

Then

$$\begin{bmatrix} v_x \\ v_y \\ v_z \end{bmatrix} = \begin{bmatrix} v_X \\ v_Y \\ v_Z \end{bmatrix} = \begin{bmatrix} 1 & 0 & 0 \\ 0 & -1 & 0 \\ 0 & 0 & -1 \end{bmatrix} \begin{bmatrix} v_{X'} \\ v_{Y'} \\ v_{Z'} \end{bmatrix} = \begin{bmatrix} v_{X'} \\ -v_{Y'} \\ -v_{Z'} \end{bmatrix},$$

and by use of Bond stress transformation matrix [20],

$$\begin{bmatrix} T_5 \\ T_4 \\ T_3 \end{bmatrix} = \begin{bmatrix} T_{xz} \\ T_{yz} \\ T_{zz} \end{bmatrix} = \begin{bmatrix} T_{XZ} \\ T_{YZ} \\ T_{ZZ} \end{bmatrix} = \begin{bmatrix} -T_{X'Z'} \\ T_{Y'Z'} \\ T_{Z'Z'} \end{bmatrix} = \begin{bmatrix} -T_{5'} \\ T_{4'} \\ T_{3'} \end{bmatrix}. \tag{18}$$

The acoustic field equations are [20]

$$\nabla \cdot \boldsymbol{T} = \rho \frac{\partial \boldsymbol{v}}{\partial t}, \qquad C : \nabla_s \boldsymbol{v} = \frac{\partial \boldsymbol{T}}{\partial t} + e : \frac{\mathrm{d}\boldsymbol{E}}{\mathrm{d}t}, \tag{19}$$

where '.' and ':' denote the summations with respect to the suffixes such as i, j, or I, J, which have occurred earlier. The damping of materials to acoustic waves is omitted while the piezoelectric effect is considered here. In this paper, $\partial/\partial z \neq 0$ as the acoustic field changes merely with the z coordinate axis.

From equations (16) and (19), We can obtain that there are only X-polarized shear waves propagating along the Z-axis in the transducer, acoustic switch and transmission medium when a pure X-polarized shear wave is excited in the transducer. Thus there are only X-polarized shear waves propagating along the Z-axis in our designed device.

Generally speaking, shear waves do not introduce volume change to medium. So, the dilation is

$$\Delta = \frac{\Delta V}{V} = 0. \tag{20}$$

Then, the relative change of the mass density is

$$\frac{\Delta \rho}{\rho} = -\frac{\Delta V}{V} = 0. \tag{21}$$

This means that there is no change of density. That is, there will be no change of mass density in the three parts of the integrated device if only shear waves propagate along the integrated device.

According to Christoffel's equation, the X-polarized shear waves propagating along the Z-axis have the velocity $\sqrt{(C_{44} - g_{244}E_2)/\rho}$ in the acoustic switch, and the velocities of shear waves both in the transducer and in the single domain LN equal $\sqrt{C_{44}/\rho}$.

2.3. The acoustic reflection by domain walls of the acoustic switch part

In this section, the reflectivity of the acoustic waves is calculated by use of the transfer-matrix method [21]. We denote a as the thickness of positive domain, and b as that of negative domain. The equation of motion of X-polarized shear wave is

$$\frac{\partial^2 u_x}{\partial t^2} = \frac{C'_{55}}{\rho'} \frac{\partial^2 u_x}{\partial z^2}, \tag{22}$$

where u_x represents the displacement, and $C'_{55} = C_{44} - g_{244}E_2$. So C'_{55} has a different values in the positive domain and the negative domain in the presence of an external electric field E_2 as g_{244} has a different sign in them. Therefore, the velocity

$$(v)_{X\text{-polarized}} = \sqrt{\frac{C'_{55}}{\rho'}}$$

will change its value when the shear waves are propagating in different domains.

The general solution of equation (22) can be written as

$$u_x(z, t) = u_x \exp(\mathrm{i}\omega t), \tag{23}$$

with

$$u_x = A_i \sin[k_i(z - z_i)] + B_i \cos[k_i(z - z_i)], \tag{24}$$

where A_i and B_i are complex constants, and the position z is in the ith domain, and z_i is the coordinate of the interface between the ith and the (i-1)th domain. The wave vector k_i is k_1 in the positive domains and k_2 in the negative domains respectively.

The boundary conditions at interface z_{i+1} (i is given an odd number here) yield

$$\begin{aligned} A_i \sin(k_1 a) + B_i \cos(k_1 a) &= B_{i+1}, \\ F[A_i \cos(k_1 a) - B_i \sin(k_1 a)] &= A_{i+1}, \end{aligned} \tag{25}$$

with

$$F = \frac{k_1 v^2}{k_2 v'^2}, \tag{26}$$

where v and v' are the velocities of the X-polarized shear wave in the positive domains and negative domains, respectively. At the same time, at the interface z_{i+2}, to satisfy the boundary conditions, we have

$$\begin{aligned} A_{i+1} \sin(k_2 b) + B_{i+1} \cos(k_2 b) &= B_{i+2}, \\ A_{i+1} \cos(k_2 b) - B_{i+1} \sin(k_2 b) &= F A_{i+2}. \end{aligned} \tag{27}$$

From equations (25) and (27), we can be obtain the following transfer-matrix form:

$$\begin{bmatrix} A_{i+2} \\ B_{i+2} \end{bmatrix} = T_i \begin{bmatrix} A_i \\ B_i \end{bmatrix}, \tag{28}$$

with

$$T_i = \begin{bmatrix} \cos(k_2 b)/F & -\sin(k_2 b)/F \\ \sin(k_2 b) & \cos(k_2 b) \end{bmatrix} \times \begin{bmatrix} F\cos(k_1 a) & -F\sin(k_1 a) \\ \sin(k_1 a) & \cos(k_1 a) \end{bmatrix}. \tag{29}$$

Considering there are $2N$ domains in the acoustic switch part. Then the amplitudes of the X-polarized shear waves at the first domain and the $(2N-1)$th domain are related by

$$\begin{bmatrix} A_{2N-1} \\ B_{2N-1} \end{bmatrix} = T'_{\text{total}} \begin{bmatrix} A_1 \\ B_1 \end{bmatrix}, \tag{30}$$

with

$$T'_{\text{total}} = \left(\prod_{i=1}^{N-1} T_{2i-1} \right).$$

The function $u_x(z)$ in the last domain of the transducer part and the single domain LN part can be written as

$$u_x = \begin{cases} \exp[\mathrm{i}k_0(z - z_0)] + p \exp[-\mathrm{i}k_0(z - z_0)] \\ \qquad \text{when } z \leqslant z_0, \\ q \exp[\mathrm{i}k_0(z - z_{2N})] \qquad \text{when } z \geqslant z_{2N}, \end{cases} \tag{31}$$

where p and q are constants, and z_0 and z_{2N} are the coordinates of the two ends of the acoustic switch. The wave vector of the shear wave in the transducer equals that in the single domain part. So we use one symbol k_0 to represent it.

From the boundary conditions at the ends, we have

$$\begin{aligned} 1 + p &= B_1, \\ \mathrm{i}(1 - p)F_1 &= A_1, \\ q &= A_{2N} \sin(k_2 b) + B_{2N} \cos(k_2 b), \\ \mathrm{i}q &= [A_{2N} \cos(k_2 b) - B_{2N} \sin(k_2 b)]F_2, \end{aligned} \tag{32}$$

with

$$F_1 = \frac{k_0 v_0^2}{k_1 v^2} \qquad \text{and} \qquad F_2 = \frac{k_2 v'^2}{k_0 v_0^2},$$

where v_0 is the velocity of waves in the transducer and in the single domain LN.

According to equations (25), (29) and (30), we have

$$\begin{bmatrix} A_{2N} \cos(k_2 b) - B_{2N} \sin(k_2 b) \\ A_{2N} \sin(k_2 b) + B_{2N} \cos(k_2 b) \end{bmatrix} = \begin{bmatrix} F & 0 \\ 0 & 1 \end{bmatrix} T_{\text{total}} \begin{bmatrix} A_1 \\ B_1 \end{bmatrix}, \tag{33}$$

with

$$T_{\text{total}} = \left(\prod_{i=1}^{N} T_{2i-1} \right).$$

From equations (32) and (33), noting that $F = 1/(F_1 F_2)$, we obtain

$$p = \frac{T_{12} + T_{21} F_1^2 + \mathrm{i}F_1(T_{11} - T_{22})}{T_{21} F_1^2 - T_{12} + \mathrm{i}F_1(T_{11} + T_{22})}, \tag{34}$$

where $T_{ij}(i, j = 1, 2)$ is the element of the matrix T_{total}. So the sound power reflectivity of the shear wave is

$$|p|^2 = \frac{(T_{12} + T_{21} F_1^2)^2 + F_1^2 (T_{11} - T_{22})^2}{(T_{21} F_1^2 - T_{12})^2 + F_1^2 (T_{11} + T_{22})^2}. \tag{35}$$

3. Discussion

From the above calculation and analysis, the advantages of our design are obvious. First, the electromechanical coefficient (0.76) is the largest among the excited modes of ASLLN [9]. Second, the ultrasonic waves are excited by 'crossed-field' scheme. This makes monolithic integration possible and thus the processes to build the devices are simpler than the conventional ones.

The new device can be fabricated by two popular methods. One is the electric field poling at room temperature, which can control domain period accurately and be operated conveniently. Gnewuch *et al* have fabricated devices through monolithic integration with this method successfully [11, 17]. The other is the Czochralski method with a certain chemical element doped into the melt [6, 16, 22–25]. The ASLLN can be fabricated by rotating the seed in an asymmetrical temperature field or by applying a modulated electric current through the solid–liquid interface during crystal growth.

For PPLN crystals, $C_{44} = 0.6 \times 10^{11}\,\mathrm{N\,m^{-2}}$, $\rho = 4.64 \times 10^3\,\mathrm{kg\,m^{-3}}$, and g_{244} is chosen as $10.15\,\mathrm{N\,V^{-1}m^{-1}}$ following [26] with the symmetric relationships described in [19]. From equation (35), we can see that the reflectivity $|p|^2$ is related with the frequency $f(= \omega/2\pi)$, the number of periods N, the domain thickness a and b, and the electric field E_2.

With further calculation, we obtain the influence of the configuration of the acoustic switch upon the reflectivity. Figure 4 shows four types of configurations of the switch. Table 1 gives the results corresponding to the number of periods $N = 2000$, the electric field $E_2 = 5.0\,\mathrm{KV\,mm^{-1}}$. It can be seen that the reflectivity values of configuration 1 are the same as those of configuration 2; it does not occur between configurations 3 and 4. But the frequency spectrum distributions are all the same for all types. The sound power reflection and transmission coefficients are $|r|^2 = (Z_2 - Z_1)^2/(Z_2 + Z_1)^2$, and $|t|^2 = 4Z_1 Z_2/(Z_2 + Z_1)^2$, where Z_1 and Z_2 are specific acoustic impedance [27]. For a plane wave, we have $Z_i = \rho_i v_i$ $(i = 1, 2)$, which represent the characteristic impedance of the medium. So the differences among the four configurations result from the different numbers of domains and different characteristic impedances of the positive and negative domains in the acoustic switch, the transducer and the transmission medium.

Figure 5 shows the dependence of the frequency spectrum distribution on the thickness of domains. To a certain domain thickness, the frequency intervals between the nearest peaks are equal. The intervals are shortened when the thickness of domains increases. From the data shown in table 1, the centre frequency of reflection peaks can be expressed as $f_{\text{s}}^m = m\bar{v}/[2(a + b)]$ $(m = 1, 3, 5, \ldots)$ for $a = b$, where $\bar{v} = (v + v')/2 \approx v_0$, and $v_0 = 3596\,\mathrm{m\,s^{-1}}$ in our case. We can see that this relation satisfies Bragg formula. The frequency difference between two adjacent peaks is $\Delta f_{\text{s}} = v/(a + b)$, in agreement with figure 6.

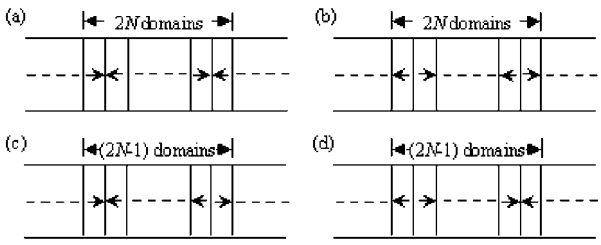

Figure 4. Configurations of the acoustic switch: (*a*) configuration 1, (*b*) configuration 2, (*c*) configuration 3 and (*d*) configuration 4. The arrows represent domains.

Table 1. The calculated reflectivities R1 and R2 corresponding to configurations $a = b = 5\,\mu$m and $a = b = 15\,\mu$m, respectively, and periods of switch.

Reflection frequency (MHz)	Configuration 1		Configuration 2		Configuration 3		Configuration 4	
	R1	R2	R1	R2	R1	R2	R1	R2
60	0	0.016 24	0	0.016 24	0	0.016 15	0	0.015 97
179.8	0.872 96	0.872 43	0.872 96	0.872 43	0.872 86	0.872 33	0.872 66	0.872 13
299.8	0	0.014 16	0	0.014 17	0	0.014 16	0	0.014 15
419.5	0	0.071 41	0	0.071 4	0	0.071 59	0	0.071 95
539.4	0.872 43	0.867 57	0.872 43	0.867 57	0.872 33	0.867 47	0.872 13	0.867 26
659.3	0	0.044 61	0	0.044 61	0	0.044 46	0	0.044 17
779.1	0	0.205 59	0	0.205 58	0	0.205 78	0	0.206 16
899	0.871 37	0.857 25	0.871 37	0.857 25	0.871 27	0.857 15	0.871 07	0.856 94

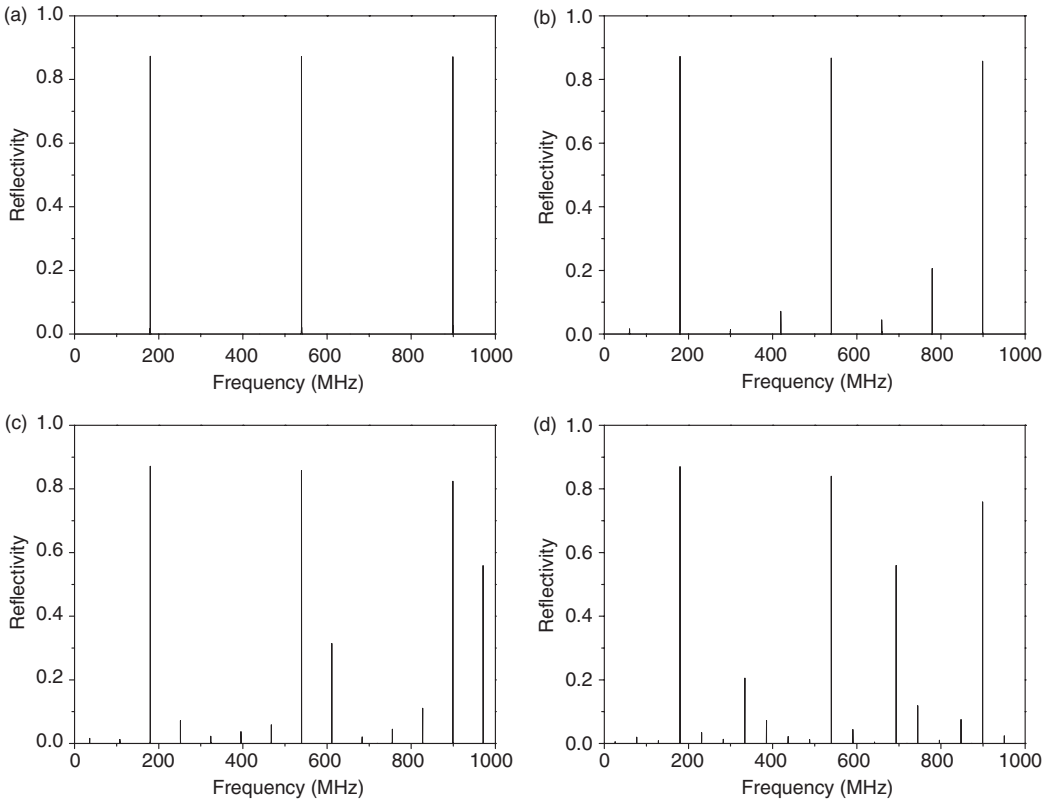

Figure 5. Reflectivity spectra of the acoustic switch for (*a*) $a = b = 5\,\mu$m, (*b*) $a = b = 15\,\mu$m, (*c*) $a = b = 25\,\mu$m and (*d*) $a = b = 35\,\mu$m. The number of periods is $N = 2000$, and the electric field $E_2 = 5.0\,\mathrm{kV\,mm^{-1}}$. The positions of distinct peaks are marked with f_s^l ($l = 1, 3, 5, \ldots$).

To find out the relation between the period of the acoustic switch and that of the transducer, we assume that in the transducer the thickness of positive and negative domains is c and d, respectively. According to [7, 9] the acoustic waves excited by the transducer have the frequency $f_t^n = nv_0/(c+d)$ ($n = 1, 2, 3, \ldots$) when $c \neq d$, or $f_t^{n'} = n'v_0/(2c)$ ($n' = 1, 3, 5, \ldots$) with $c = d$. When $f_s^m = f_t^n$ (or $f_t^{n'}$), i.e. $c + d = 2n(a+b)/m$ (or $c = n'(a+b)/m$), the reflection of the acoustic switch happens. For example, when $c \neq d$, if $c + d = 2(a + b)$, the acoustic waves with the frequency $f_t^l = lv_0/(c+d)$ ($l = 1, 3, 5, \ldots$) excited in the transducer will be reflected by the acoustic switch.

Figures 6 and 7 show the influence of the electric field E_2 and the number of periods N upon the reflectivity, respectively. Some examples are given in tables 2 and 3. It can be seen that the greater the E_2 (or N), the greater the reflectivity. The bandwidth increases with E_2 while decreases with N. We can see that the sound power reflection coefficient $|r|^2$ increases with the characteristic impedance difference $|Z_2 - Z_1|$. In section 2.2, we have already deduced the velocity of the acoustic wave $v = \sqrt{(C_{44} - g_{244}E_2)/\rho}$. Since $g_{244}E_2/C_{44}$ is small, $v = \sqrt{(C_{44} - g_{244}E_2)/\rho} = \sqrt{C_{44}/\rho}[1 - g_{244}E_2/(2C_{44})] = v_0 - \Delta v$, where $v_0 = \sqrt{C_{44}/\rho}$, and $\Delta v = v_0 g_{244}E_2/(2C_{44})$ with g_{244} being positive in positive domains and negative in negative domains. Therefore $|r|^2$ will increase with Δv, i.e. it will increase with E_2. In addition, a large contrast in velocities between the positive and negative domains will result in large acoustic bandgaps as can be seen in figure 6. That is, by changing the external electric field E_2 we can modify both the reflectivity and the bandwidth of the integrated device.

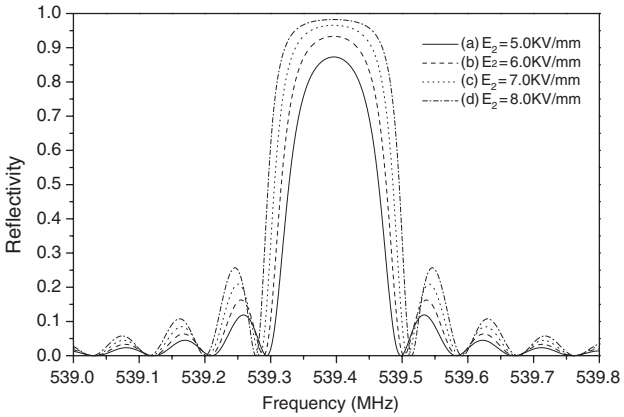

Figure 6. Reflectivity spectra of the acoustic switch for (*a*) $E_2 = 5.0\,\mathrm{kV\,mm^{-1}}$, (*b*) $E_2 = 6.0\,\mathrm{kV\,mm^{-1}}$, (*c*) $E_2 = 7.0\,\mathrm{kV\,mm^{-1}}$ and (*d*) $E_2 = 8.0\,\mathrm{kV\,mm^{-1}}$. The number of periods is $N = 2000$, and the thickness of domains $a = b = 5\,\mu$m.

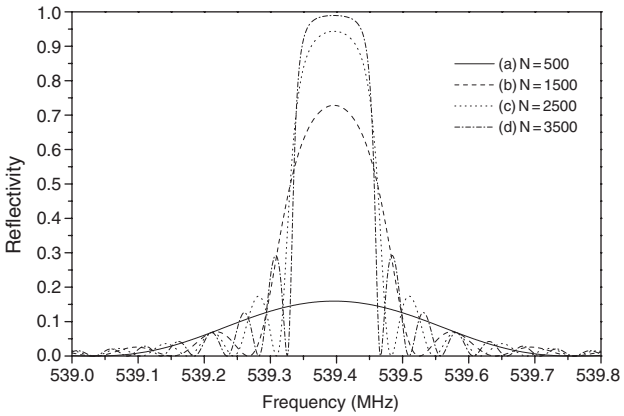

Figure 7. Reflectivity spectra of the acoustic switch for (*a*) $N = 500$, (*b*) $N = 1500$, (*c*) $N = 2500$ and (*d*) $N = 3500$. The thickness of domains $a = b = 5\,\mu$m, and the electric field $E_2 = 5.0\,\mathrm{kV\,mm^{-1}}$.

Table 2. The calculated reflectivity and bandwidth for two different external fields when $N = 2000$, and $a = b = 5\,\mu$m.

E_2 ($\mathrm{kV\,mm^{-1}}$)	Reflectivity	Bandwidth (kHz)
5.0	0.876	120
7.0	0.966	160

Table 3. The calculated reflectivity and bandwidth for two different numbers of periods when $a = b = 5\,\mu$m and $E_2 = 5.0\,\mathrm{kV\,mm^{-1}}$.

N	Reflectivity	Bandwidth (kHz)
1500	0.729	130
2500	0.943	120

4. Summary

An integrated acoustic device, including a transducer, an acoustic switch, and a transmission medium, is proposed. The propagation of the acoustic waves in the device is analysed theoretically considering the influence of an external electric field. The elastoelectric coefficient, being a fifth-rank tensor, is modulated periodically in PPLN. This results in the velocity differences of acoustic waves in the positive and the negative domains.

For an acoustic switch made of PPLN, the reflectivity is a function with respect to the frequency of the acoustic wave, the thickness of domains, the velocity of the acoustic wave, and the external electric field. Frequencies up to 1000 MHz have been discussed. The distribution expression of reflectivity spectra is consistent with Bragg formula with the ratio of the period of the acoustic switch to that of the transducer being $m/(2n)$ ($m = 1, 3, 5, \ldots$, $n = 1, 2, 3, \ldots$ or $1, 3, 5\ldots$). The reflection ability of the acoustic switch is strengthened and the acoustic bandgaps are broadened with the increase of the external electric field, whereas, in the absence of DC bias, there will be no obstructions to acoustic waves. According to the quantitative results of the reflectivity and the distribution of reflectivity spectra, it is possible to design a switchable reflector based on PPLN. The experiments are being carried out.

Acknowledgment

This work was supported by a grant for the State Key Program for Basic Research of China, by the National Natural Science Foundation of China (no 69938010 and 19920041).

References

[1] Feng D, Ming N B, Hong J F, Zhu J S, Yang Z and Wang Y N 1980 *Appl. Phys. Lett.* **37** 607
[2] Lu Y Q, Wan Z L, Wang Q, Xi Y X and Ming N B 2000 *Appl. Phys. Lett.* **77** 3719
[3] Blistanov A A, Danilov A A, Rodionov D A, Sorokin N G, Turkov Y G and Chizhikov S I 1986 *Sov. J. Quantum Electron.* **16** 1678
[4] Lu Y Q, Xiao M and Salamo G J 2001 *Appl. Phys. Lett.* **78** 1035
[5] Zhu Y Y, Ming N B, Jiang W H and Shui Y A 1988 *Appl. Phys. Lett.* **53** 2278
[6] Zhu Y Y, Ming N B, Jiang W H and Shui Y A1988 *Appl. Phys. Lett*. **53** 1381
[7] Zhu Y Y and Ming N B 1992 *J. Appl. Phys.* **72** 904
[8] Zhu Y Y, Chen Y F, Zhu S N, Qin Y Q and Ming N B 1996 *Mater. Lett.* **28** 503
[9] Zhu Y Y, Zhu S N, Qin Y Q and Ming N B 1996 *J. Appl. Phys.* **79** 2221
[10] Zhu Y Y, Zhu S N and Ming N B 1996 *J. Phys. D: Appl. Phys*. **29** 185
[11] Gnewuch H, Zayer N K and Pannell C N 2000 *IEEE Trans. Ultrasonics, Ferroelectrics, and Frequency Control* **47** 1619
[12] Alshits V I, Darinskiy A N, Shuvalov A L, Antipov V V, Chizhikov S I and Sorokin N G 1989 *Ferroelectrics* **96** 351
[13] Smith W R, Gerard H M, Collins J H, Reeder T M and Shaw H J 1969 *IEEE Trans. Microwave Theory Tech.* **17** 856
[14] Sitting E K 1969 *IEEE Trans. Son. Ultroson.* **16** 2
[15] Chen Y F, Zhu S N, Zhu Y Y, Ming N B, Jin B B and Wu R X 1997 *Appl. Phys. Lett.* **70** 592
[16] Cheng S D, Zhu Y Y, Lu Y L and Ming N B 1995 *Appl. Phys. Lett*. **66** 291
[17] Gnewuch H, Zayer N K, Pannell C N, Ross G W and Smith P G R 2000 *Opt. Lett*. **25** 305
[18] Niizeki N, Yamada T and Toyoda H 1967 *Japan. J. Appl. Phys.* **6** 318
[19] Chizhikov S I, Sorokin N G. and Petrakov V S 1988 *Piezoelectrics* 75

[20] Auld B A 1973 *Acoustic Fields and Waves in Solids* vol 1 (New York: Wiley)
[21] Dong H and Xiong S J 1993 *J. Phys.: Condens. Matter* **5** 8849
[22] Ming N B, Hong J F and Feng D 1982 *J. Mater. Sci*. **17** 1663
[23] Wan Z L, Wang Q, Xi Y X, Lu Y Q, Zhu Y Y and Ming N B 2000 *Appl. Phys. Lett*. **77** 1891
[24] Lu Y L, Mao L, Cheng S D, Ming N B and Lu Y T 1991 *Appl. Phys. Lett.* **59** 516
[25] Feisst A and Koidl P 1985 *Appl. Phys. Lett*. **47** 1125
[26] Cho Y and Yamanouchi K1987 *J. Appl. Phys.*. **61** 875
[27] Blackstock D T 2000 *Fundamentals of Physical Acoustics* (New York: Wiley) pp 110–12